Journal of Materials Chemistry B

RSC Publishing

PAPER

View Article Online
View Journal | View Issue

Cite this: J. Mater. Chem. B, 2013, 1, 5347

Platinum nanodendrite functionalized graphene nanosheets as a non-enzymatic label for electrochemical immunosensing

Qiunan Xu, Lisong Wang, Jianping Lei,* Shengyuan Deng and Huangxian Ju*

Received 24th March 2013
Accepted 20th May 2013

DOI: 10.1039/c3tb20410c

www.rsc.org/MaterialsB

An ultrasensitive immunosensing method was developed using platinum nanodendrite functionalized graphene nanosheets (PtNDs@GS) as a non-enzymatic label for the electrochemical detection of human immunoglobulin G (HIgG). The PtNDs@GS hybrid was prepared *in situ* by reducing K_2PtCl_4 with ascorbic acid in an aqueous solution of reduced graphene oxide, and characterized by scanning electron microscopy, transmission electron microscopy and spectral techniques. The disposable immunosensor was constructed by coating a polyethylene glycol film on a screen-printed carbon working electrode and then immobilizing the capture antibody on the film. After binding with the antigen for further capture of the PtNDs@GS labelled antibody, PtNDs@GS was introduced as an electrochemical tag to produce a large electrocatalytic current towards the reduction of dissolved oxygen for signal amplification. Compared with the enzyme-based immunosensor, PtNDs@GS as non-enzymatic tag exhibited many advantages. This method showed a good linearity in the concentration range of 1 pg mL^{-1} to 10 ng mL^{-1}, with a detection limit of 0.87 pg mL^{-1}. PtNDs@GS as non-enzymatic label provides a versatile method for constructing ultrasensitive immunosensors, and demonstrates proof-of-concept in immunosensing.

Introduction

Ultrasensitive immunoassays for biomarkers have attracted considerable interest in biomedical research and clinic diagnostics, especially in early-disease screening and diagnosis.[1–3] In order to realize ultrasensitivity, many signal amplification strategies have been designed using molecular biology and nanomaterial-based amplification techniques.[4–16] Due to their large surface-to-volume ratio and excellent conductivity,[17–20] nanomaterials such as carbon- and metal-based nanoparticles are promising candidates for carriers to load a large number of signal molecules for amplifying the recognition event. For example, by using carbon nanotubes (CNTs) as a carrier to immobilize enzymes, a general amplification strategy combined with electrochemical detection has been developed for the highly sensitive detection of prostate-specific antigen with a detection limit of 4 pg mL^{-1}.[21] When coupled to superparamagnetic beads massively loaded with about 500 000 horseradish peroxidase labels and secondary antibodies, an unprecedented detection limit of 1 fg mL^{-1} (100 aM) was achieved for the detection of interleukin 8.[22] Although those methods demonstrated high sensitivity, the easy denaturation of enzymes in natural environments and need for a nitrogen atmosphere block their applications in practice.

To avoid the deoxygenation process, the direct electrochemical signal of metallic nanoparticles, including gold nanoparticles[23] and silver nanoparticles,[24] has been used for ultrasensitive immunoassay. For example, streptavidin-functionalized silver-nanoparticle-enriched CNTs have been designed as a trace tag to obtain a sensitive electrochemical-stripping signal for the multiplexed immunoassay of carcinoembryonic antigen (CEA) and α-fetoprotein (AFP).[25] The electrocatalytic activity of metal nanoparticles such as platinum nanoparticles,[26] palladium nanoparticles[27] and metal alloys[28–31] can also be used to realize ultrasensitive immunoassay. By the catalytic reduction of *p*-nitrophenol to *p*-aminophenol using gold nanocatalyst labels, a simple electrochemical method for signal amplification has been achieved for the sensitive detection of mouse IgG.[32] Here, the excellent conductivity of graphene was combined with the strong catalytic ability of platinum nanoparticles to form platinum nanodendrite functionalized graphene nanosheets (PtNDs@GS), producing an electrocatalytic label for construction of an ultrasensitive immunosensing strategy.

Platinum nanoparticles are efficient catalysts for both oxygen reduction and methanol oxidation.[33–36] In particular, graphene nanosheet supported platinum nanoparticles are one of the most attractive systems in catalysis research due to their remarkable catalytic capacity and free electron mobility.[37–39] In

State Key Laboratory of Analytical Chemistry for Life Science, School of Chemistry and Chemical Engineering, Nanjing University, Nanjing 210093, P. R. China. E-mail: jpl@nju.edu.cn; hxju@nju.edu.cn; Fax: +86 25 83593593; Tel: +86 25 83593593

this work, based on the high electrocatalytic activity of PtNDs@GS towards the reduction of dissolved oxygen, a disposable electrochemical immunosensor was proposed for the ultrasensitive detection of human immunoglobulin G (HIgG) (Scheme 1). The immunosensor was constructed by coating a polyethylene glycol (PEG) film on screen-printed carbon working electrodes (SPCEs) and then immobilizing the capture antibody (Ab_1) on the film. With a sandwich-type immunoassay format, the analyte and then the PtNDs/GS-labeled antibody were successively captured to the immunocomplex to obtain the amplified electrocatalytic signal for readout. Using dissolved oxygen as the signal reporter, the detection process avoided deoxygenation and showed excellent analytical performance with good fabrication reproducibility, and acceptable precision and accuracy. The PtNDs@GS as a non-enzymatic label provides a versatile approach for the design of ultrasensitive immunosensing methods.

Experimental

Reagents and materials

Human IgG (HIgG) and polyclone rabbit anti-human IgG antibody (RaHIgG) were purchased from Wuhan Boster Biological Technology Ltd. Potassium tetrachloroplatinate(II) (K_2PtCl_4, 99.99%) and bovine serum albumin (BSA) were obtained from Sigma-Aldrich Chemical Co. (St. Louis, MO). Polyvinylpyrrolidone K-30, (PVP, M_w = 40 000), polyethylene glycol (PEG, M_w = 20 000), hydrazine hydrate and ascorbic acid were obtained from Sinopharm Chemical Reagent Co., Ltd (Shanghai, China). All other reagents were of analytical grade and used as received. Ultrapure water obtained from a Millipore water purification system (≥18 MΩ, Milli-Q, Millipore) was used in all assays. 0.1 M phosphate-buffered saline (PBS) solutions with various pHs were prepared by mixing stock solutions of NaH_2PO_4 and Na_2HPO_4. PBS (pH 7.4) containing 50 mg mL^{-1} BSA was used as the blocking buffer. The immunosensor was kept at 4 °C when not in use.

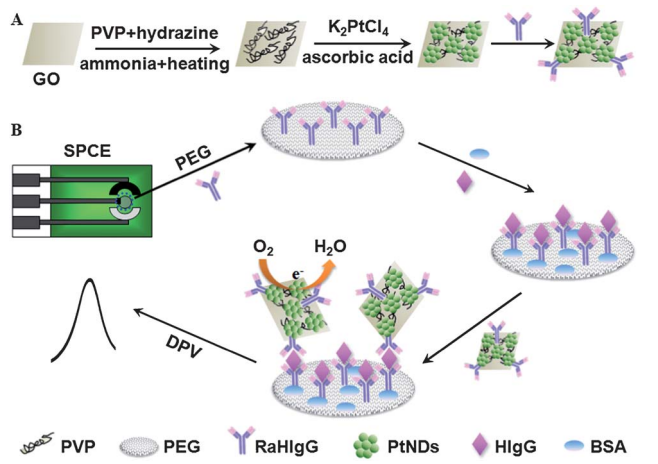

Scheme 1 Schematic representation of (A) the preparation of PtNDs@GS-labeled RaHIgG and (B) the signal amplification strategy for sensitive electrochemical immunoassay.

Characterization

Transmission electron microscope (TEM) images were obtained using a JEM-2100 TEM instrument (Hitachi, Japan) with an accelerating voltage of 200 kV for high-resolution TEM images after drop-casting the sample dispersion onto a carbon coated 300 mesh copper grid and drying under room temperature. Attenuated total reflection (ATR)-FTIR spectra were recorded on a Vector 22 FTIR spectrometer (Bruker Optics, Germany). X-ray photoelectron spectroscopy (XPS) experiments were carried out on an ESCALAB 250 spectrometer (Thermo-VG Scientific Co., USA) with ultra-high vacuum generators. Differential pulse voltammetric (DPV) measurements were performed using a CHI 660C electrochemical workstation (CH Instruments Inc., USA).

Preparation of PVP-GS

Graphene oxide (GO, ~1.1 μm × 1.2 μm) was synthesized from graphite by a modified Hummers method.[40] Then a 50 mL aqueous dispersion of as-prepared GO (0.5 mg mL^{-1}) was sonicated for 40 min, and centrifuged (3000 rpm) to remove non-exfoliated GO sheets. 400 mg PVP was added to the dispersion and stirred overnight to obtain a PVP-GO dispersion. 35 μL of hydrazine (50% w/w) and 400 μL of ammonia (25% w/w) were injected into the resulting solution with vigorous stirring for several minutes, and then the solution was maintained at 95 °C for 1 h to obtain black reduced graphene oxide (GS). After centrifugation, the resulting black product was purified by washing in water three times, and redispersed in water to yield 2.0 mg mL^{-1} of the PVP-GS dispersion.

Preparation of PtNDs@GS nanohybrid

500 μL of 2 mg mL^{-1} PVP-GS was diluted to 3.8 mL in a 10 mL flask, and then mixed completely with 250 μL of 1 M PVP and 1.45 mL of 0.2 M ascorbic acid. The mixture was heated to 95 °C with magnetic stirring in an oil bath. Next, 0.5 mL 0.1 M K_2PtCl_4 solution was rapidly injected into the flask, and the mixture was kept at 95 °C for 3 hours. After cooling to room temperature, the product was collected by centrifugation, washed several times with water, and redispersed in water to obtain the PtNDs@GS nanohybrid for further electrochemical measurements.

Labeling of PtNDs@GS to RaHIgG

200 μL of the as-prepared PtNDs@GS was first diluted to 1 mL with water. Then RaHIgG (10 μL, 1.0 mg mL^{-1}) was added into the solution, followed by gentle shaking at room temperature for 1 h. During this process, RaHIgG could be loaded onto the PtNDs through physical adsorption and the interactions between the mercapto or amino groups of RaHIgG and the PtNDs. After washing with PBS (pH 6.0) three times, and centrifugation, the soft sediment was rinsed with PBS containing BSA (5%) at 4 °C for 0.5 h. The conjugate was finally centrifuged and resuspended in PBS (200 μL) containing BSA (0.1%) for immunoassay.

Fabrication of the immunosensor

The SPCE, containing carbon working electrode (2 mm in diameter), carbon auxiliary electrode and Ag/AgCl reference electrode, was fabricated according to the steps reported previously.[41] The insulating layer printed around the working area constituted a reservoir of the electrochemical cell with a volume of 50 μL.

The PEG film modified electrode was first prepared by dropping 5 μL of 2.0 mg mL^{-1} PEG solution onto the working electrode. The chip was incubated in a water vapor saturated environment at 4 °C overnight to allow the passive adsorption of PEG onto the carbon electrode surface. The PEG not only assisted the antibody immobilization, but also minimized nonspecific adsorption. After washing with water, 1 μL of 0.2 mg mL^{-1} RaHIgG antibody in PBS (pH 7.4) was dropped on the PEG film and incubated for 40 min at 25 °C to allow the assembly of the antibody. Then, the electrode surface was washed with water and incubated with 50 μL 5% BSA for 1 h to block possible remaining active sites against nonspecific adsorption. Finally, the immunosensor was rinsed with water and stored at 4 °C in dry air in the dark prior to use.

Immunoassay procedure

A sandwich-type immunoassay was performed for detection. The immunosensor was first incubated with 5 μL of the sample containing HIgG for 40 min at 25 °C. After a washing step with ultrapure water using a pipettor, 5 μL of the PtNDs@GS labeled RaHIgG was cast on the immunosensor for 45 min incubation at 25 °C. After washing with water, 50 μL of PBS was dropped onto the electrochemical microcell to perform the DPV detection from +0.1 to −0.5 V, with a step potential of 4 mV, a pulse amplitude of 50 mV, and a pulse period of 0.2 s.

Results and discussion

The PtNDs@GS was prepared by *in situ* deposition of PtNPs on the surface of PVP encapsulated GS. Fig. 1 displays the TEM images of PVP-GS and PtNDs@GS at different magnifications. The TEM image revealed flexible few-layer wrinkled sheets of the PVP-GS situated on the top of the copper grid (Fig. 1A), illustrating the flake-like shape of GS. Using ascorbic acid as a reduction reagent, K_2PtCl_4 could be reduced to PtNDs and homogeneously distributed on the GS surface with a diameter of around 45 nm (Fig. 1B and C). Fig. 1D shows the fine structure of the PtNDs, which were constructed from thousands of Pt nanoparticles with a 2 nm diameter, and possessed a typical structure of clusters, internal clearance and a huge surface area-to-weight ratio. The enriched deposition of PtNDs would promote the reduction of oxygen, and the GS carrier would improve the loading of PtNDs on the sensor surface, as well as providing a feasible pathway for electron transfer due to its remarkable conductivity. These properties should permit the construction of an electrocatalytic platform for biosensing.

Through the interaction of the thiol and amino functional groups of antibody molecules with noble metal nanoparticles,[42] the adsorptive immobilization of RaHIgG antibody onto PtNDs should be a simple and effective means for stably attaching the biomolecules and retaining the specific immunorecognition ability. Fig. 2A shows the reflectance absorption IR spectra of PtNDs@GS and PtNDs@GS labeled RaHIgG. Compared with the spectrum of PtNDs@GS (curve a), PtNDs@GS labeled RaHIgG showed the typical vibrations of amide I and amide II of the protein at 1524 and 1630 cm^{-1} (curve b),[9] indicating the successful assembly of RaHIgG on the tracing tag.

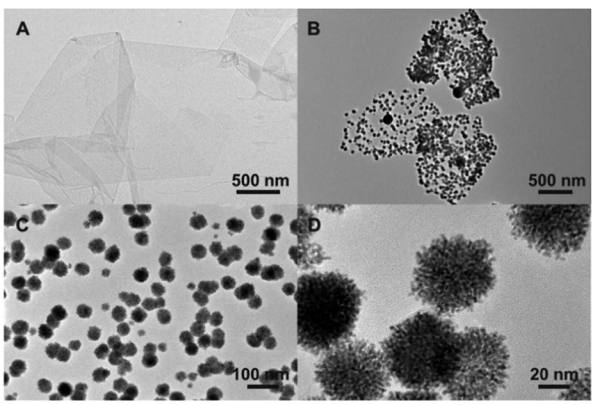

Fig. 1 TEM images of (A) PVP-GS, (B) PtNDs@GS. (C) and (D) are the amplifications of (B) at two different scales.

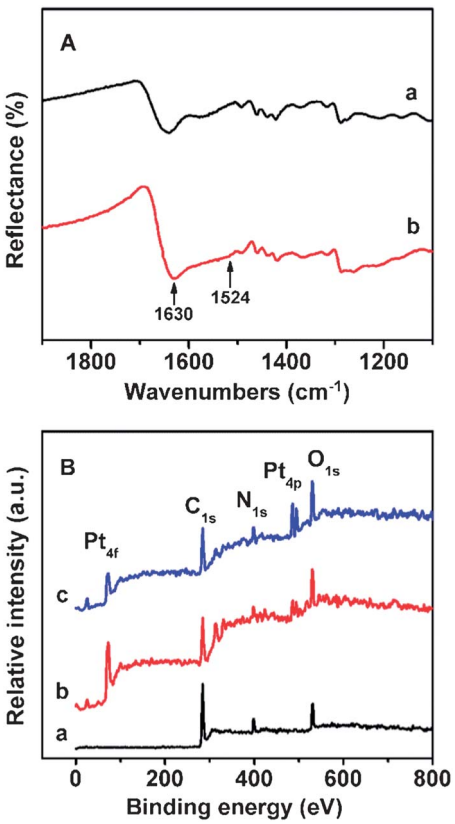

Fig. 2 (A) IR spectra of (a) PtNDs@GS and (b) PtNDs@GS labeled RaHIgG. (B) XPS spectra of (a) PVP-GS, (b) PtNDs@GS, and (c) PtNDs@GS labeled RaHIgG.

The successful assembly of RaHIgG on PtNDs@GS was also verified by XPS spectroscopy (Fig. 2B). The spectrum of PVP-GS shows distinct C 1s, N 1s and O 1s peaks (curve a). On the other hand, the spectrum of PtNDs@GS shows a pair of strong new peaks at 72.6 eV and 519.6 eV (curve b), which represent Pt 4f and Pt 4p, respectively, indicating the existence of Pt element in the nanohybrid. Compared with PtNDs@GS, the spectrum of PtNDs@GS labeled RaHIgG shows an increase in the relative contents of elements C, N and O, with a decline in the relative content of Pt (curve c), consistent with the assembly of protein on the tracing tag.

The electrocatalytic activity of PVP-GS, PtNDs@GS and PtNDs@GS labeled RaHIgG towards the reduction of oxygen was investigated by DPV measurements (Fig. 3). In the studied potential window, the PtNDs@GS modified SPCE showed a sensitive DPV peak at −0.15 V after 50 μL of air-saturated PBS was cast on the electrode surface (curve a), while PVP-GS modified SPCE showed no obvious peak in air-saturated PBS (curve b). After the adsorptive immobilization of RaHIgG, the PtNDs@GS labeled RaHIgG modified SPCE showed a slightly low DPV peak in air-saturated PBS (curve c), which derived from the non-conductive protein wrapping around the outer layer of the tracing tag. Meanwhile, in N_2-saturated PBS, no electrocatalytic current was observed in the PtNDs@GS labeled RaHIgG modified SPCE (curve d). These results indicate that the largely amperometric response should be contributed to by the catalytic reduction of dissolved O_2 by PtNDs to H_2O through a four-electron process.[33] The relatively strong catalytic ability of PtNDs@GS labeled RaHIgG as an electrochemical tag was expected to achieve highly sensitive biosensing.

In order to achieve optimal analytical performance of the immunoassay, the incubation conditions were optimized. The concentration of labeled antibody affected the extent and speed of immunoreaction. Fig. 4A shows the effect of concentration of the PtNDs@GS labeled RaHIgG on the DPV response. At 25 °C with an incubation time of 45 min, the peak current increased with the increasing concentration of labeled antibody from 0.1 to 0.2 mg mL^{-1}, and reached a maximum value at 0.2 mg mL^{-1}. Beyond 0.2 mg mL^{-1}, the peak current gradually decreased. Thus, 0.2 mg mL^{-1} was selected as the optimal incubation concentration for the sandwich immunoassay, at which the incubation time was optimized. As shown in Fig. 4B, the DPV response reached a maximum value at the incubation time of 45 min, indicating the saturated binding of the immunoreactions. A longer time led to excess protein being bound to the sensor surface and decreased the conductivity. Therefore, 45 min was chosen as the optimal incubation time.

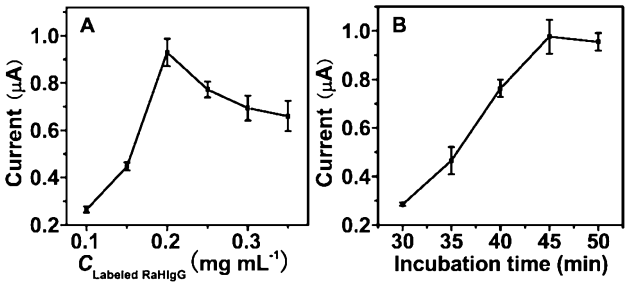

Fig. 4 Effects of (A) concentration of the PtNDs@GS labeled RaHIgG and (B) incubation time of the detection solution on the DPV response to 5 ng mL^{-1} HIgG at the immunosensor.

The use of the GS carrier offered a high amount of PtNDs on each immunoconjugate and provided a feasible pathway for electron transfer, and hence amplified the detectable signal from the electro-reaction of dissolved oxygen. Under the optimal detection conditions, the DPV peak current of the immunosensor after incubation with HIgG and PtNDs@GS labeled RaHIgG increased with increasing HIgG concentration, which resulted in an increasing amount of PtNDs captured on the immunosensors (Fig. 5). Thus, the reduction peak potential shifted to more positive values with the increasing HIgG concentration. Meanwhile, the calibration plot showed a good linear relationship between the peak current (peak height after subtraction of the background) and the logarithmic value of the HIgG concentration ranging from 1 pg mL^{-1} to 10 ng mL^{-1}, with a correlation coefficient of 0.985. The detection limit corresponding to the current signal of three times the standard deviation obtained from five current measurements in the absence of HIgG was approximately 0.87 pg mL^{-1}, which was much lower than the limits of 4.4 ng mL^{-1} for the magnetic bead based chemiluminescence resonance energy transfer immunoassay,[43] 50 pg mL^{-1} for a gold nanoparticle/GS based electrochemical immunosensor,[44] and 10 pg mL^{-1} for a quantum dot based electrochemiluminescent immunosensor.[45]

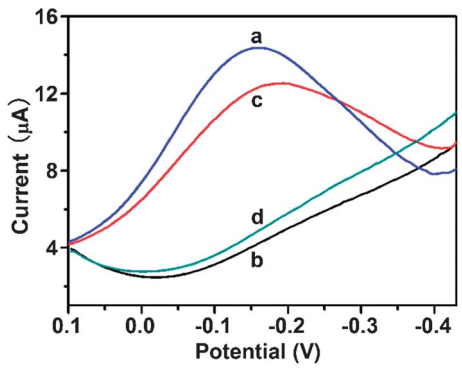

Fig. 3 DPV responses of SPCEs modified with 5 μL of (a) as-prepared PtNDs@GS and (b) 2.0 mg mL^{-1} PVP-GS in air-saturated PBS, and the PtNDs@GS labeled RaHIgG bound SPCEs in (c) air- and (d) N_2-saturated PBS.

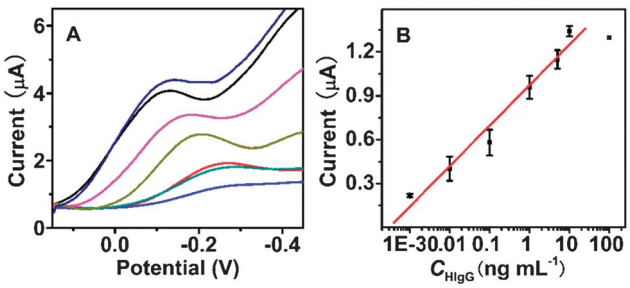

Fig. 5 (A) DPV responses to 0.001, 0.01, 0.1, 1, 5, 10 and 100 ng mL^{-1} HIgG (from bottom to top) using the proposed immunosensor. (B) Calibration curve.

The specificity of the immunosensor was examined by testing its DPV responses to interfering substances, such as BSA, CEA, AFP, and glucose prepared in blank PBS. The responses of the immunosensor to 10 mg mL^{-1} BSA, 100 ng mL^{-1} CEA, 100 ng mL^{-1} AFP, and 1 mM glucose were between 0.042 and 0.065 μA, which were near to that of the blank PBS (0.053 ± 0.04 μA), and much smaller than that of 0.1 ng mL^{-1} HIgG (0.49 ± 0.03 μA), indicating the good specificity of the proposed immunosensor. These results also indicated that the PEG modified SPCE had good feasibility for the detection of serum samples.[46]

The inter-assay precision of the immunosensor was evaluated by using five chips. The coefficients of variation were 7.3% and 4.6% for 0.5 and 5 ng mL^{-1} HIgG, indicating acceptable precision and fabrication reproducibility. After the immunosensors were stored in dry air in the dark at 4 °C for two weeks, 93.2% of the initial DPV response for HIgG remained. Thus, the immunosensor possessed acceptable stability. These results suggested that the immunosensor holds significant potential for application in clinical analysis.

Conclusion

This work designed PtNDs functionalized GS as an electrochemical label to develop a highly sensitive disposable immunosensor. Combining the excellent conductivity of GS with the strong catalytic ability of PtNDs, the designed tracing tag of PtNDs@GS demonstrated excellent electrocatalytic activity towards the reduction of oxygen. Moreover, the use of a GS carrier offered a high loading amount of PtNDs on each immunoconjugate, and hence amplified the detectable signal from the electro-reduction of dissolved oxygen. Using dissolved oxygen as a signal reporter, the detection process avoided deoxygenation and additional signal molecules. Under optimal conditions, the immunosensor achieved a low detection limit, down to sub-picomolar levels. In addition, the immunosensor showed excellent analytical performance with good fabrication reproducibility, acceptable stability, precision and accuracy, and showed potential for applications in clinical diagnosis. The PtNDs@GS as non-enzymatic labels hold great promise in the construction of electrochemical immunoassay methods, and demonstrates proof-of-concept in signal-amplification strategies for the ultrasensitive detection of biomarkers.

Acknowledgements

This work was financially supported by the National Basic Research Program of China (2010CB732400) and the National Natural Science Foundation of China (21075060, 21121091, 21135002).

Notes and references

1 S. K. Arya and S. Bhansali, *Chem. Rev.*, 2011, **111**, 6783.
2 J. P. Lei and H. X. Ju, *Chem. Soc. Rev.*, 2012, **41**, 2122.
3 B. Zhang, D. P. Tang, I. Y. Goryacheva, R. Niessner and D. Knopp, *Chem.–Eur. J.*, 2013, **19**, 2496.
4 H. X. Ju, *J. Biochips Tissue Chips*, 2012, **2**, 1000e114.
5 J. A. Ho, Y. C. Lin, L. S. Wang, K. C. Hwang and P. T. Chou, *Anal. Chem.*, 2009, **81**, 1340.
6 L. Y. Chen, C. L. Chen, R. N. Li, Y. Li and S. Q. Liu, *Chem. Commun.*, 2009, 2670.
7 H. X. Ju, *Sci. China: Chem.*, 2011, **54**, 1202.
8 R. M. Alhotra, V. Patel, J. P. Vaqué, J. S. Gutkind and J. F. Rusling, *Anal. Chem.*, 2010, **82**, 3118.
9 J. Zhang, J. P. Lei, C. L. Xu, L. Ding and H. X. Ju, *Anal. Chem.*, 2010, **82**, 1117.
10 D. Du, Z. X. Zou, Y. S. Shin, J. Wang, H. Wu, M. H. Engelhard, J. Liu, I. A. Aksay and Y. H. Lin, *Anal. Chem.*, 2010, **82**, 2989.
11 W. S. Qu, Y. Y. Liu, D. B. Liu, Z. Wang and X. Y. Jiang, *Angew. Chem., Int. Ed.*, 2011, **50**, 3442.
12 G. F. Jie, L. Wang and S. S. Zhang, *Chem.–Eur. J.*, 2011, **17**, 641.
13 R. Akter, M. A. Rahman and C. K. Rhee, *Anal. Chem.*, 2012, **84**, 6407.
14 J. Q. Liu, T. Song, Q. H. Yang, J. Tan, D. H. Huang and J. Chang, *J. Mater. Chem. B*, 2013, **1**, 1156.
15 X. Cao, N. Wang, S. Jia, L. Guo and K. Li, *Biosens. Bioelectron.*, 2013, **39**, 226.
16 B. Jeong, R. Akter, O. H. Han, C. K. Rhee and M. A. Rahman, *Anal. Chem.*, 2013, **85**, 1784.
17 J. B. Liu, S. H. Fu, B. Yuan, Y. L. Li and Z. X. Deng, *J. Am. Chem. Soc.*, 2010, **132**, 7279.
18 S. Krishnan, V. Mani, D. Wasalathanthri, C. V. Kumar and J. F. Rusling, *Angew. Chem., Int. Ed.*, 2011, **50**, 1175.
19 B. V. Chikkaveeraiah, A. A. Bhirde, N. Y. Morgan, H. S. Eden and X. Y. Chen, *ACS Nano*, 2012, **6**, 6546.
20 M. Perfezou, A. Turner and A. Merkoçi, *Chem. Soc. Rev.*, 2012, **41**, 2606.
21 X. Yu, B. Munge, V. Patel, G. Jensen, A. Bhirde, J. D. Gong, S. N. Kim, J. Gillespie, J. S. Gutkind, F. Papadimitrakopoulos and J. F. Rusling, *J. Am. Chem. Soc.*, 2006, **128**, 11199.
22 B. S. Munge, A. L. Coffey, J. M. Doucette, B. K. Somba, R. Malhotra, V. Patel, J. S. Gutkind and J. F. Rusling, *Angew. Chem., Int. Ed.*, 2011, **50**, 7915.
23 C. Leng, G. S. Lai, F. Yan and H. X. Ju, *Anal. Chim. Acta*, 2010, **666**, 97.
24 B. P. Ting, J. Zhang, M. Khan, Y. Y. Yang and J. Y. Ying, *Chem. Commun.*, 2009, 6231.
25 G. S. Lai, J. Wu, H. X. Ju and F. Yan, *Adv. Funct. Mater.*, 2011, **21**, 2938.
26 S. J. Guo, D. Wen, Y. M. Zhai, S. J. Dong and E. K. Wang, *ACS Nano*, 2010, **4**, 3959.
27 R. Polsky, J. C. Harper, D. R. Wheeler, S. M. Dirk, J. A. Rawlings and S. M. Brozik, *Chem. Commun.*, 2007, 2741.
28 Y. Song, Y. T. Ma, Y. Wang, J. W. Di and Y. F. Tu, *Electrochim. Acta*, 2010, **55**, 4909.
29 B. Lim, M. J. Jiang, P. H. C. Camargo, E. C. Cho, J. Tao, X. M. Lu, Y. M. Zhu and Y. N. Xia, *Science*, 2009, **324**, 1302.
30 S. J. Guo, S. J. Dong and E. K. Wang, *ACS Nano*, 2010, **4**, 547.
31 Q. Wei, Y. F. Zhao, B. Du, D. Wu, Y. Y. Cai, K. X. Mao, H. Li and C. X. Xu, *Adv. Funct. Mater.*, 2011, **21**, 4193.

32 J. Das, M. A. Aziz and H. Yang, *J. Am. Chem. Soc.*, 2006, **128**, 16022.
33 Y. Liu and W. E. Mustain, *J. Am. Chem. Soc.*, 2013, **135**, 530.
34 F. J. Vidal-Iglesias, A. López-Cudero, J. Solla-Gullón and J. M. Feliu, *Angew. Chem., Int. Ed.*, 2013, **52**, 964.
35 S. J. Kwon and A. J. Bard, *J. Am. Chem. Soc.*, 2012, **134**, 10777.
36 L. Hutton, M. E. Newton, P. R. Unwin and J. V. Macpherson, *Anal. Chem.*, 2009, **81**, 1023.
37 L. Estevez, A. Kelarakis, Q. M. Gong, E. H. Da'as and E. P. Giannelis, *J. Am. Chem. Soc.*, 2011, **133**, 6122.
38 Y. J. Li, Y. J. Li, E. B. Zhu, T. McLouth, C. Y. Chiu, X. Q. Huang and Y. Huang, *J. Am. Chem. Soc.*, 2012, **134**, 12326.
39 B. P. Vinayan, R. Nagar and S. Ramaprabhu, *J. Mater. Chem.*, 2012, **22**, 25325.
40 N. I. Kovtyukhova, P. J. Ollivier, B. R. Martin, T. E. Mallouk, S. A. Chizhik, E. V. Buzaneva and A. D. Gorchinskiy, *Chem. Mater.*, 1999, **11**, 771.
41 J. Wu, Z. J. Zhang, Z. F. Fu and H. X. Ju, *Biosens. Bioelectron.*, 2007, **23**, 114.
42 J. Zhang, J. P. Lei, R. Pan, C. Leng, Z. Hu and H. X. Ju, *Chem. Commun.*, 2011, **47**, 668.
43 G. X. Qin, S. L. Zhao, Y. Huang, J. Jiang and F. G. Ye, *Anal. Chem.*, 2012, **84**, 2708.
44 K. P. Liu, J. J. Zhang, C. M. Wang and J. J. Zhu, *Biosens. Bioelectron.*, 2011, **26**, 3627.
45 X. Liu, Y. Y. Zhang, J. P. Lei, Y. D. Xue, L. X. Cheng and H. X. Ju, *Anal. Chem.*, 2010, **82**, 7351.
46 Q. N. Xu, F. Yan, J. P. Lei, C. Leng and H. X. Ju, *Chem.–Eur. J.*, 2012, **18**, 4994.